http://www.jstage.jst.go.jp/browse/biophysics

BIOPHYSICS

REVIEW

Vol. 9, pp. 51–56 (2013)
doi: 10.2142/biophysics.9.51

Rotary catalysis of F_oF_1-ATP synthase

Rikiya Watanabe[1]

[1]*Department of Applied Chemistry, School of Engineering, The University of Tokyo, Bunkyo-ku, Tokyo 113-8656, Japan*

Received March 28, 2013; accepted April 22, 2013

The synthesis of ATP, the key reaction of biological energy metabolism, is accomplished by the rotary motor protein; F_oF_1-ATP synthase (F_oF_1). *In vivo*, F_oF_1, located on the cell membrane, carries out ATP synthesis by using the proton motive force. This heterologous energy conversion is supposed to be mediated by the mechanical rotation of F_oF_1; however, it still remained unclear. Recently, we developed the novel experimental setup to reproduce the proton motive force *in vitro* and succeeded in directly observing the proton-driven rotation of F_oF_1. In this review, we describe the interesting working principles determined so far for F_oF_1 and then introduce results from our recent study.

Key words: ATP synthase, molecular motor, heterogeneous energy conversion

F_oF_1 ATP synthase (F_oF_1) is a molecular energy-converter which catalyzes physiologically important synthesis of ATP from ADP and inorganic phosphate (P_i) by using the electrochemical energy in proton gradient; the proton motive force (*pmf*) across bio-membranes[1–3]. The prominent feature of F_oF_1 is that mechanical rotation of the inner rotor complex mediates the aforementioned heterologous energy conversion with high efficiency and reversibility[4,5], which is not found in other biological systems, and therefore, F_oF_1 attracts great interest from many researchers across a wide range of research fields. F_oF_1 comprises 2 rotary motors, F_1 and F_o (Fig. 1a). F_1 ($\alpha_3\beta_3\gamma\delta\varepsilon$), a water-soluble part of F_oF_1, is an ATP-driven rotary motor, which couples ATP hydrolysis or synthesis at $\alpha_3\beta_3\delta$ stator ring to the mechanical rotation of $\gamma\varepsilon$ complex in counterclockwise direction (Fig. 1b)[6]. Each $\alpha\beta$ interface possesses a catalytic site for ATP hydrolysis[7]; F_1 hydrolyzes 3 ATP molecules per turn[8]. Extensive studies have been done to understand the chemo-mechanical coupling mechanism of F_1[9–18], and therefore, currently, F_1 is one of the best characterized molecular motor proteins.

F_o, a membrane-embedded part of F_oF_1, is the proton-driven rotary motor, which couples proton translocation to mechanical rotation of the oligomer ring of the *c*-subunit against the ab_2 complex (Fig. 1b)[5,19,20]. Each *c*-subunit has a proton-binding site and mediates proton translocation: 1 proton per *c*-subunit per rotation. Thus, the number of *c*-subunits in the *c*-ring is thought to determine the total number of protons translocated per rotation. While the number of *c*-subunits varies among species from 8 to 15[21,22], the bacterial F_o, such as *E-coli* and thermophilic *Bacillus* PS3, has 10 *c*-subunits that form a c_{10}-ring[23,24]. It is difficult to handle F_o since it is embedded in the membrane, and therefore, the rotary mechanism of F_o remains elusive.

In a cell, F_1 and F_o are connected via central and peripheral stalks (Fig. 1a), which allow the torque transmission between the 2 motors. Under physiological conditions, F_o generates a larger torque than F_1 and reverses the rotary direction of F_1, thereby inducing the reverse reaction of ATP hydrolysis, *i.e.* ATP synthesis (Fig. 2a). In contrast, when *pmf* diminishes, F_1 hydrolyzes ATP and reverses the rotary direction of F_o, thereby enforcing pumping of protons by F_o in order to generate *pmf* (Fig. 2b). Thus, F_oF_1 manifests reversibility with regard to the process of energy conversion, and the rotation of inner rotor complex plays an important role in this reversibility.

To understand the precise role of the rotation on the energy conversion of F_oF_1, some single-molecule studies have been carried out[5,19,20,25–27]. Due to ease of handling, ATP-driven rotation of detergent-solubilized F_oF_1, which is

Corresponding author: Rikiya Watanabe, Department of Applied Chemistry, School of Engineering, The University of Tokyo, Bunkyo-ku, Tokyo 113-8656, Japan.
e-mail: wrikiya@nojilab.t.u-tokyo.ac.jp

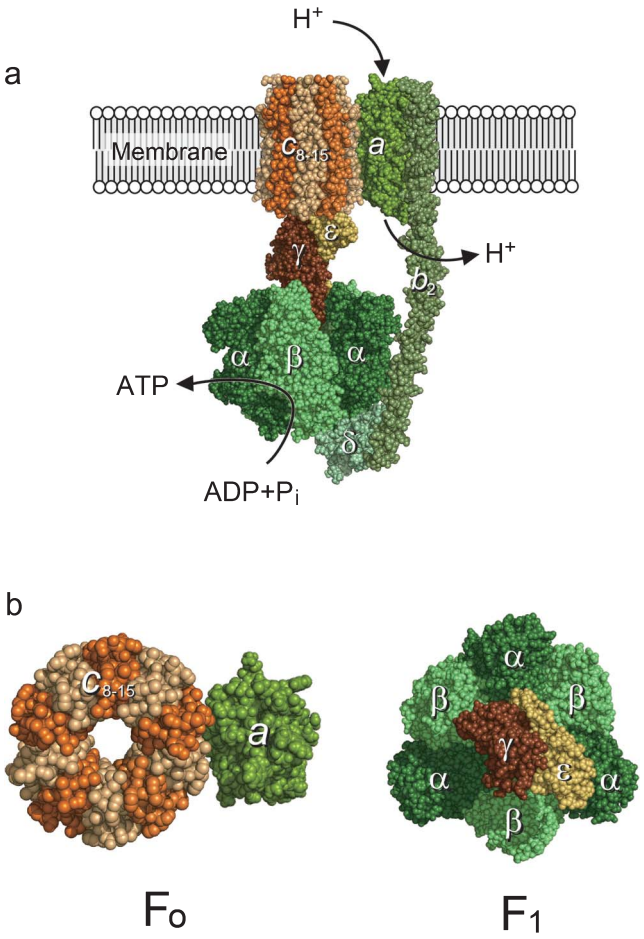

Figure 1 Structural model of bacterial F_oF_1-ATP synthase (a) The space-filling model of F_oF_1 (side view) is assembled from several partial structures obtained by X-ray crystallography and NMR (PDB codes 1C17, 1B9U, 2KHK, 1L2P, 3UDO, 3OAA, and 1ABV). F_oF_1 has subunit stoichiometry of $\alpha_3\beta_3\gamma\delta\varepsilon ab_2c_{8-15}$. F_oF_1 is composed of 2 rotary motors; a membrane-embedded F_o (ab_2c_{8-15}) and a water-soluble F_1 ($\alpha_3\beta_3\gamma\delta\varepsilon$). Proton flows through the channels located at the *a*–*c* interface of F_o, while ATP synthesis is carried out at the catalytic sites located at the α–β interface of F_1. (b) Top view of F_o (left) and F_1 (right).

no longer part of a bio-membrane, has been studied; however, *pmf*-driven rotation has not been studied sufficiently. In this year, we developed a novel experimental setup that for the first time allowed direct observation of the proton-driven rotation of F_oF_1 [20]. In this review, we focus on the role of rotary motion in the energy conversion of F_oF_1, and introduce the fundamental working principles determined so far, including the results from our recent study[20].

Energy conversion mechanism

As mentioned above, ATP synthesis/hydrolysis reaction is reversibly coupled with proton translocation across the membrane. To understand the reversible energy conversion mechanism of F_oF_1, extensive biochemical studies have been performed. Since it is difficult to measure the time course of *pmf* generated by F_oF_1, most studies pertained to the measurement of ATP synthesis activity under a given *pmf*. In general, *pmf* mainly comprises 2 components: the trans-membrane proton gradient (ΔpH) and the potential difference (Δψ). At first, biochemical studies examined ATP synthesis activity by changing the amplitude of each of these components of *pmf*, and examined the component-dependence of ATP synthesis activity of F_oF_1 [28–34]. In recent studies, F_oF_1 was purified and reconstituted into liposomes, and the ATP synthesis rate was quantitatively measured by the acid–base transition or valinomycin-mediated K^+ diffusion potential for producing ΔpH or Δψ. It was found that ΔpH and Δψ contribute equally to ATP synthesis rate of F_oF_1, and, moreover, either ΔpH or Δψ alone can drive synthesis of ATP[29]. Kinetic equivalence implies that F_oF_1 can use ΔpH or Δψ to drive rotation at an equal efficiency.

Next, to determine the coupling efficiency in F_oF_1, biochemical studies examined the number of protons translocated per synthesis of 1 molecule of ATP; the H^+/ATP ratio, by enzymes from various organisms, e.g., *Escherichia coli*, yeast, and chloroplasts[4,35,36]. In view of the rotary catalysis model of F_oF_1, the H^+/ATP ratio should coincide with the ratio of the number of proton-binding *c*-subunits to the 3 catalytic nucleotide-binding β-subunits when proton-translocation and ATP synthesis are highly coupled. Analyses of the equilibrium point, where the free energy of ATP synthesis is balanced with that of proton translocation, allowed determination of the H^+/ATP ratio. The determined H^+/ATP ratios were dependent on the stoichiometry of the *c* and β subunits, although they were not identical to the *c*/β ratios. In particular, H^+/ATP ratios in a recent study were smaller than the *c*/β ratios[36], which implies that proton translocation is stochastically coupled to the synthesis of ATP; however, the coupling efficiency is extremely high.

ATP-driven rotation

To understand the precise role of rotation in the energy conversion, the rotation of F_oF_1 was observed at single-molecule level. At first, due to the ease of handling, ATP-driven rotation of solubilized F_oF_1 from *E. coli* and thermophilic *Bacillus* PS3 was observed (Fig. 3)[25,26,37]. In this condition where F_oF_1 was not a part of membrane, *pmf* was not imposed on F_oF_1, and F_o did not generate the rotary torque. Therefore, as same as isolated F_1, F_oF_1 rotated in a counterclockwise direction, and showed a 120°-stepping rotation at low ATP concentrations, in which ATP binding was the rate-limiting step of rotation. This 120°-stepping rotation reflects the structural symmetry of F_1; 3 catalytic sites for ATP hydrolysis/synthesis are located on a single molecule of F_1[7].

Next, the rotation of F_oF_1 reconstituted in a membrane was observed. Ishmukhametov et al. developed an experimental setup with a gold nanorod and phospholipid bilayer nanodisc, which has been shown to provide a good model

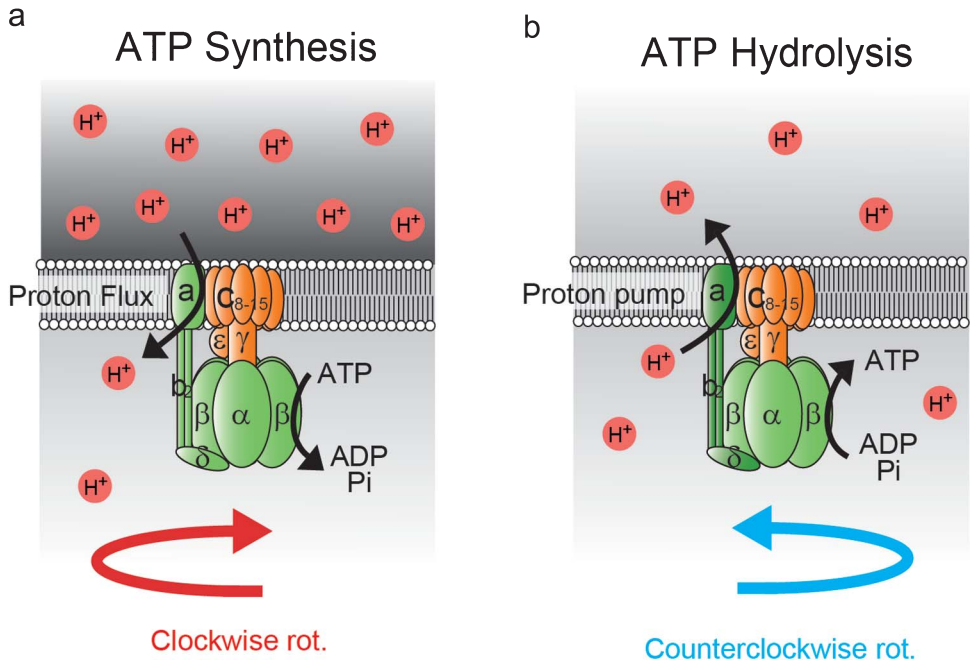

Figure 2 Heterologous energy conversion by F_oF_1
Energy conversion mechanism of F_oF_1 in ATP synthesis (a) or hydrolysis (b) conditions. Orange and light green represent the rotor and stator subcomplex, respectively.

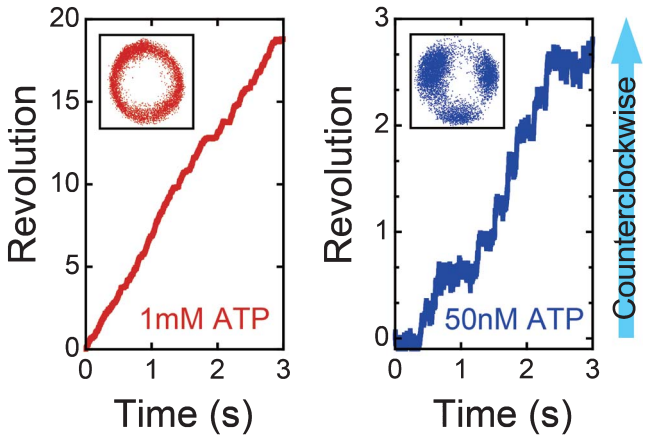

Figure 3 ATP-driven rotation of F_oF_1
Time course of the ATP-driven rotation of solubilized F_oF_1 in the presence of 1 mM ATP (left) and 50 nM ATP (right). The insets show the centroid trajectories of the rotating particles. At low ATP concentration, F_oF_1 showed a 120° stepping rotation.

for a lipid bilayer membrane, and attempted to visualize the rotary motion of membrane-constituted *E. coli* F_oF_1 driven by ATP hydrolysis[27]. In their setup, the gold nanorod was attached to the *c*-subunit as a rotation probe. The intensity of scattered red light from a nanorod changes in a sinusoidal manner as a function of the rotary position, and therefore, the rotary motion of F_oF_1 could be visualized from the analysis of red light scattered from the nanorod. On the other hand, the F_o module was buried within the phospholipid bilayer nanodisc, which is large enough to allow incorporation of F_o, but which is on the same scale as the F_oF_1 complex, and thus, it was difficult to generate a *pmf* across the nanodisc. Using this experimental setup, the 36° stepping rotation of F_oF_1 in the presence of a high concentration of polyethylene glycol was observed for the first time. This reflects the structural symmetry of the F_o module; 10 proton binding sites are located on a single molecule of F_o[24]. In this setup, as mentioned above, *pmf* was not imposed on F_oF_1, and F_o did not generate rotary torque; and therefore, it could not be confirmed whether the 36° step was coupled to the translocation of protons.

pmf-driven rotation

Diez et al. developed a method to indirectly visualize the rotation of *E. coli* F_oF_1 that had been reconstituted in liposomes by using single molecule Förster resonance energy transfer (sm-FRET)[5]. In their method, they introduced a pair of FRET probes at a stator and rotor subunit of F_oF_1 for visualization of the rotary motion of F_oF_1, and generated the *pmf* by using the acid–base transition or valinomycin-mediated K^+ diffusion potential method, as mentioned above. By using this method, they observed the 120° stepping rotation driven by ATP hydrolysis[5], and moreover, for the first time observed the obscure 36° stepping rotation driven by *pmf* [19]. However, due to the low signal-to-noise ratio and fast photobleaching of the fluorescent dyes used in sm-FRET, high resolution tracking and long-term recording of the rotational dynamics of F_oF_1 has not yet been achieved (recording time < approximately 300 ms). Therefore, the

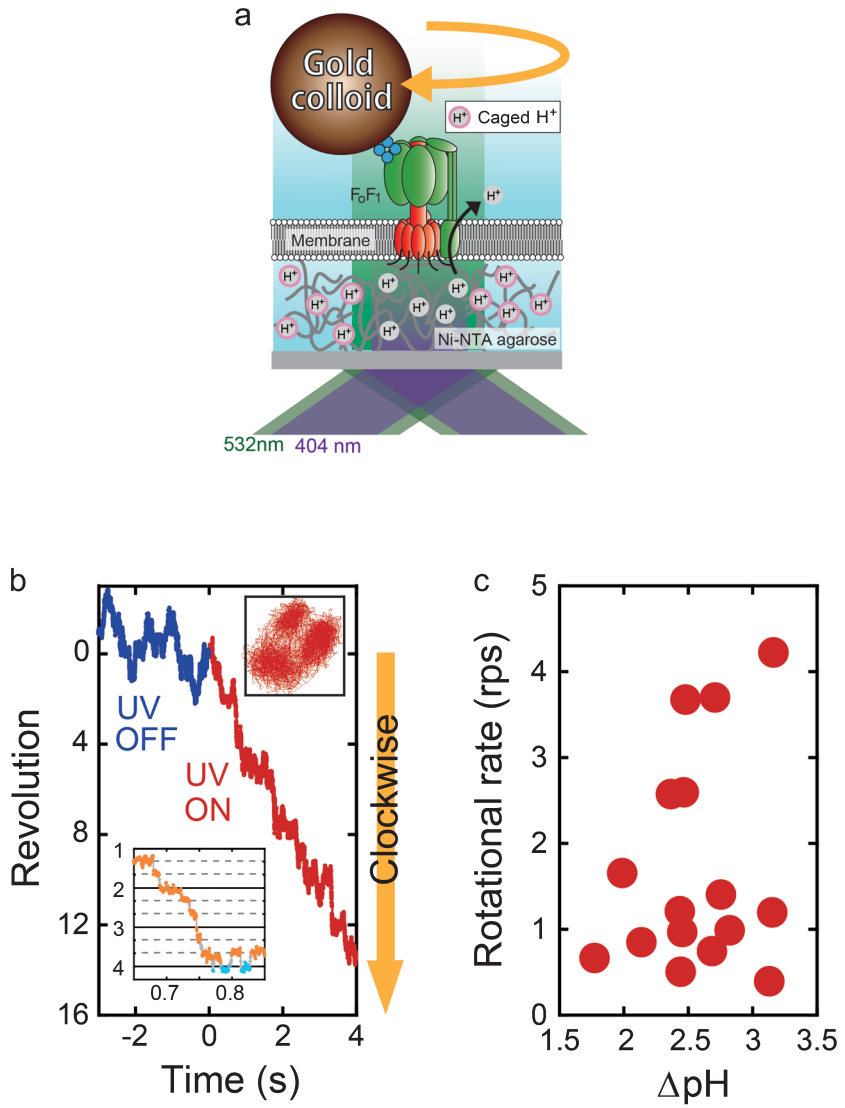

Figure 4 Proton-driven rotation of F_oF_1

(a) Schematic model of the novel experimental setup used to directly visualize the proton-driven rotation of F_oF_1. Evanescent illumination by 532-nm and 404-nm lasers was used. (b) Time course of the proton-driven rotation of F_oF_1 in the presence of 50 μM ADP, 1 μM ATP, and 200 μM P_i before (blue) and after (red) UV irradiation. The left inset shows an enlarged view of the time course. Orange and light blue points represent the pauses before clockwise and counterclockwise steps, respectively. The right inset shows the centroid trajectory of the rotating particle during UV irradiation. Under these conditions, F_oF_1 showed the stochastic 120° stepping rotation. (c) Rotational speed plotted against the trans-membrane proton gradient (ΔpH).

fundamental features of the *pmf*-driven rotation of F_oF_1, such as the exact step size, unidirectionality of the rotation, and stochasticity of the steps, has remained elusive to date.

To solve this problem, we recently developed a novel experimental setup that allows long-term direct observation of the *pmf*-driven rotation of *E. coli* F_oF_1 with a high spatiotemporal resolution (Fig. 4a)[20]. In this setup, the F_oF_1-reconstituted, supported membrane was expanded on a coverslip covered with Ni-NTA-modified agarose, where F_oF_1 molecules were anchored via His-tags that had been introduced to the periplasmic side of the *c*-subunits. The 80-nm gold colloid was attached as a rotation probe onto the β subunits of F_1 to allow visualization using a total internal reflection dark-field illumination system, which facilitated the long-term recording of rotation (approximately 10 s) with a high spatiotemporal resolution of about 5 nm and <0.5 ms[38]. In addition, *pmf* across the supported lipid bilayer was generated by photolysis of caged protons [1-(2-Nitrophenyl) ethyl sulfate] with a total internal reflection illumination of UV light (λ=404 nm) that selectively acidified the space between the coverslip and the lipid bilayer (the interspace). This novel setup can stably generate ΔpH of 1.8–3.7 for several tens of seconds, while the conventional method, *i.e.* acid–base transition, can generate ΔpH for only a few seconds. The magnitude of ΔpH upon photolysis of the caged protons was measured using a pH-sensitive fluorescent dye,

pHrodo-Red (pHrodo)[39], which increased the fluorescent signal upon acidification.

By using this experimental setup, we for the first time observed the clockwise rotary motion of F_oF_1 upon UV irradiation (averaged velocity was 2.7 rps.), while no rotating particles were observed prior to UV irradiation (Fig. 4b). To investigate the correlation between the rotational rate and ΔpH, we measured ΔpH by using the pHrodo located at the region where F_oF_1 showed rotations. Although F_oF_1 showed a large variation in velocity, it was still evident that faster rotation occurred at higher ΔpH (Fig. 4c). In addition, the data points of higher velocity at a given ΔpH qualitatively agreed with the aforementioned biochemical measurement of ATP synthesis activity[28], showing that the rotation observed in this study was coupled to the proton translocation and ATP synthesis, and vice versa, the rotation of F_oF_1 can mediate the energy conversion with high efficiency.

We also observed a 120° stepping rotation of F_oF_1 driven by *pmf* (Fig. 4b). The step size of rotation, viz., 120°, implies that the rotary potential of F_1 with 3-fold symmetry dominated the overall rotary potential of F_oF_1. In other words, the kinetic bottleneck of the *pmf*-driven rotation was not proton-translocation in F_o, but a catalytic event(s) on F_1, such as ATP release or P_i binding[14,40]. This result is consistent with a previous sm-FRET measurement of rotation of F_oF_1 in ATP synthesis condition where a pair of FRET probes were introduced at a stator of F_o and a rotor subunit of F_1 [5], while small steps that was estimated to be 36° were recorded when FRET probes were introduced into F_o[19]. In the present study, we immobilized the rotor part of F_o on a coverslip and attached the rotation probe at the stator part of F_1. Therefore, the observed rotation reflects the stepping behavior both of F_1 and F_o as shown in the other works, in which 36°-steps of ATP-driven rotation of F_oF_1 were observed in a similar experimental setup[27]. However, we do not exclude the possibility that the difference in the probe position caused the apparently different step size of the rotation. Another possible reason for the inconsistency in step size is the difference in the components of the *pmf*; while *pmf* in the sm-FRET measurements was composed of both ΔpH and Δψ, *pmf* was essentially composed only of ΔpH in our study. To confirm this, a method for direct observation of the proton-driven rotation of F_oF_1 by applying Δψ is crucial.

On the other hand, noted that the stepping rotation of F_oF_1 was highly stochastic; F_oF_1 showed forward-and-backward (clockwise-and-counterclockwise) steps during rotation (Fig. 4b). This is a prominent feature of the *pmf*-driven rotation of F_oF_1 that is not seen in the ATP-driven rotation of F_1 or F_oF_1. Surprisingly, the stepping was also observed in the absence of *pmf*, suggesting that *pmf* biased the rotary diffusion of F_oF_1 to the clockwise direction. To confirm this, we analyzed the pause durations between the 120°-steps. In the absence of *pmf*, the histograms of the pause duration before clockwise or counterclockwise steps showed single exponential decay. The rate constants of the clockwise and counterclockwise steps were determined to be 65 and 61 s^{-1}, respectively. The equilibrium constant of clockwise rotation was, thus, almost 1. In the presence of *pmf*, the rate constant of clockwise stepping markedly increased about two-fold, while that of counterclockwise step decreased slightly. Thus, the equilibrium constant in the presence of *pmf* increased to 2, showing that *pmf* actually biased step direction. This result also suggests that chemical equilibrium was slightly biased toward ATP synthesis by *pmf*. The stochastic rotation of F_oF_1 would represent rotation under physiological conditions, where free energy of ATP synthesis almost balances *pmf*.

Future prospects

Owing to the progress of single molecule observation techniques, we can directly observe the rotary motion of F_oF_1 both in ATP hydrolysis and synthesis conditions. In particular, the introduced novel experimental setup that allows us to stably apply, under an optical microscope, *pmf* to the membrane will push forward to understand the rotary catalysis mechanism of F_oF_1 in ATP synthesis condition, which had been unclear for long time. This experimental strategy is fundamentally applicable to the study on the dynamics of other membrane proteins driven by electrochemical potential. The most promising experiment is the application of this protocol to transporters and ion channels since there are several caged compounds that release specific ions or chemicals. Such studies would reveal the generality and uniqueness of the finding in single-molecule studies on F_oF_1.

Acknowledgements

We thank Y. Moriizumi for the experiment on solubilized F_oF_1, and all members of Noji Laboratory for critical discussion. This work was supported by Grant-in-Aid for Scientific Research (No. 30540108) to R. W. from the Ministry of Education, Culture, Sports, Science and Technology, Japan.

References

1. Yoshida, M., Muneyuki, E. & Hisabori, T. ATP synthase—a marvellous rotary engine of the cell. *Nat. Rev. Mol. Cell Biol.* **2**, 669–677 (2001).
2. Junge, W., Sielaff, H. & Engelbrecht, S. Torque generation and elastic power transmission in the rotary F_oF_1-ATPase. *Nature* **459**, 364–370 (2009).
3. Weber, J. Structural biology: Toward the ATP synthase mechanism. *Nat. Chem. Biol.* **6**, 794–795 (2010).
4. Turina, P., Samoray, D. & Gräber, P. H^+/ATP ratio of proton transport-coupled ATP synthesis and hydrolysis catalysed by CF_oF_1-liposomes. *EMBO J.* **22**, 418–426 (2003).
5. Diez, M., Zimmermann, B., Börsch, M., König, M., Schweinberger, E., Steigmiller, S., Reuter, R., Felekyan, S., Kudryavtsev, V., Seidel, C. A. & Gräber, P. Proton-powered

subunit rotation in single membrane-bound F_oF_1-ATP synthase. *Nat. Struct. Mol. Biol.* **11**, 135–141 (2004).
6. Noji, H., Yasuda, R., Yoshida, M. & Kinosita, K., Jr. Direct observation of the rotation of F_1-ATPase. *Nature* **386**, 299–302 (1997).
7. Abrahams, J. P., Leslie, A. G., Lutter, R. & Walker, J. E. Structure at 2.8 Å resolution of F_1-ATPase from bovine heart mitochondria. *Nature* **370**, 621–628 (1994).
8. Yasuda, R., Noji, H., Kinosita, K., Jr. & Yoshida, M. F_1-ATPase is a highly efficient molecular motor that rotates with discrete 120 degree steps. *Cell* **93**, 1117–1124 (1998).
9. Ariga, T., Muneyuki, E. & Yoshida, M. F_1-ATPase rotates by an asymmetric, sequential mechanism using all three catalytic subunits. *Nat. Struct. Mol. Biol.* **14**, 841–846 (2007).
10. Yasuda, R., Noji, H., Yoshida, M., Kinosita, K., Jr. & Itoh, H. Resolution of distinct rotational substeps by submillisecond kinetic analysis of F_1-ATPase. *Nature* **410**, 898–904 (2001).
11. Shimabukuro, K., Yasuda, R., Muneyuki, E., Hara, K. Y., Kinosita, K., Jr. & Yoshida, M. Catalysis and rotation of F_1 motor: cleavage of ATP at the catalytic site occurs in 1 ms before 40 degree substep rotation. *Proc. Natl. Acad. Sci. USA* **100**, 14731–14736 (2003).
12. Nishizaka, T., Oiwa, K., Noji, H., Kimura, S., Muneyuki, E., Yoshida, M. & Kinosita, K., Jr. Chemomechanical coupling in F_1-ATPase revealed by simultaneous observation of nucleotide kinetics and rotation. *Nat. Struct. Mol. Biol.* **11**, 142–148 (2004).
13. Adachi, K., Oiwa, K., Nishizaka, T., Furuike, S., Noji, H., Itoh, H., Yoshida, M. & Kinosita, K., Jr. Coupling of rotation and catalysis in F_1-ATPase revealed by single-molecule imaging and manipulation. *Cell* **130**, 309–321 (2007).
14. Watanabe, R., Iino, R. & Noji, H. Phosphate release in F_1-ATPase catalytic cycle follows ADP release. *Nat. Chem. Biol.* **6**, 814–820 (2010).
15. Watanabe, R., Okuno, D., Sakakihara, S., Shimabukuro, K., Iino, R., Yoshida, M. & Noji, H. Mechanical modulation of catalytic power on F_1-ATPase. *Nat. Chem. Biol.* **8**, 86–92 (2011).
16. Adachi, K., Oiwa, K., Yoshida, M., Nishizaka, T. & Kinosita, K., Jr. Controlled rotation of the F_1-ATPase reveals differential and continuous binding changes for ATP synthesis. *Nat. Commun.* **3**, 1022 (2012).
17. Rondelez, Y., Tresset, G., Nakashima, T., Kato-Yamada, Y., Fujita, H., Takeuchi, S. & Noji, H. Highly coupled ATP synthesis by F_1-ATPase single molecules. *Nature* **433**, 773–777 (2005).
18. Itoh, H., Takahashi, A., Adachi, K., Noji, H., Yasuda, R., Yoshida, M. & Kinosita, K. Mechanically driven ATP synthesis by F_1-ATPase. *Nature* **427**, 465–468 (2004).
19. Düser, M. G., Zarrabi, N., Cipriano, D. J., Ernst, S., Glick, G. D., Dunn, S. D. & Börsch, M. 36 degrees step size of proton-driven c-ring rotation in F_oF_1-ATP synthase. *EMBO J.* **28**, 2689–2696 (2009).
20. Watanabe, R., Tabata, K. V., Iino, R., Ueno, H., Iwamoto, M., Oiki, S. & Noji, H. Biased Brownian stepping rotation of F_oF_1-ATP synthase driven by proton motive force. *Nat. Commun.* **4**, 1631 (2013).
21. Dimroth, P., von Ballmoos, C. & Meier, T. Catalytic and mechanical cycles in F-ATP synthases. Fourth in the cycles review series. *EMBO Rep.* **7**, 276–282 (2006).
22. von Ballmoos, C., Cook, G. M. & Dimroth, P. Unique rotary ATP synthase and its biological diversity. *Annu. Rev. Biophys.* **37**, 43–64 (2008).
23. Mitome, N., Suzuki, T., Hayashi, S. & Yoshida, M. Thermophilic ATP synthase has a decamer c-ring: indication of non-integer 10:3 H^+/ATP ratio and permissive elastic coupling. *Proc. Natl. Acad. Sci. USA* **101**, 12159–12164 (2004).
24. Jiang, W., Hermolin, J. & Fillingame, R. H. The preferred stoichiometry of c subunits in the rotary motor sector of Escherichia coli ATP synthase is 10. *Proc. Natl. Acad. Sci. USA* **98**, 4966–4971 (2001).
25. Sambongi, Y., Iko, Y., Tanabe, M., Omote, H., Iwamoto-Kihara, A., Ueda, I., Yanagida, T., Wada, Y. & Futai, M. Mechanical rotation of the c subunit oligomer in ATP synthase (F_oF_1): direct observation. *Science* **286**, 1722–1724 (1999).
26. Ueno, H., Suzuki, T., Kinosita, K., Jr. & Yoshida, M. ATP-driven stepwise rotation of F_oF_1-ATP synthase. *Proc. Natl. Acad. Sci. USA* **102**, 1333–1338 (2005).
27. Ishmukhametov, R., Hornung, T., Spetzler, D. & Frasch, W. D. Direct observation of stepped proteolipid ring rotation in E. coli F_oF_1-ATP synthase. *EMBO J.* **29**, 3911–3923 (2010).
28. Iino, R., Hasegawa, R., Tabata, K. V. & Noji, H. Mechanism of inhibition by C-terminal alpha-helices of the epsilon subunit of Escherichia coli F_oF_1-ATP synthase. *J. Biol. Chem.* **284**, 17457–17464 (2009).
29. Soga, N., Kinosita, K., Yoshida, M. & Suzuki, T. Kinetic Equivalence of Transmembrane pH and Electrical Potential Differences in ATP Synthesis. *J. Biol. Chem.* **287**, 9633–9639 (2012).
30. Bokranz, M., Morschel, E. & Kroger, A. Phosphorylation and phosphate-ATP exchange catalyzed by the ATP synthase isolated from Wolinella succinogenes. *Biochim. Biophys. Acta* **810**, 332–339 (1985).
31. Slooten, L. & Vandenbranden, S. ATP-synthesis by proteoliposomes incorporating Rhodospirillum rubrum F_oF_1 as measured with firefly luciferase: dependence on delta psi and delta pH. *Biochim. Biophys. Acta* **976**, 150–160 (1989).
32. Junesch, U. & Gräber, P. The rate of ATP-synthesis as a function of delta pH and delta psi catalyzed by the active, reduced H^+-ATPase from chloroplasts. *FEBS Lett.* **294**, 275–278 (1991).
33. Wiedenmann, A., Dimroth, P. & von Ballmoos, C. Functional asymmetry of the F_o motor in bacterial ATP synthases. *Mol. Microbiol.* **72**, 479–490 (2009).
34. Fischer, S. & Graber, P. Comparison of ΔpH- and Δψ-driven ATP synthesis catalyzed by the H^+-ATPases from Escherichia coli or chloroplasts reconstituted into liposomes. *FEBS Lett.* **457**, 327–332 (1999).
35. Steigmiller, S., Turina, P. & Graber, P. The thermodynamic H^+/ATP ratios of the H^+-ATPsynthases from chloroplasts and Escherichia coli. *Proc. Natl. Acad. Sci. USA* **105**, 3745–3750 (2008).
36. Petersen, J., Forster, K., Turina, P. & Gräber, P. Comparison of the H^+/ATP ratios of the H^+-ATP synthases from yeast and from chloroplast. *Proc. Natl. Acad. Sci. USA* **109**, 11150–11155 (2012).
37. Tsunoda, S. P., Aggeler, R., Yoshida, M. & Capaldi, R. A. Rotation of the c subunit oligomer in fully functional F_1F_o ATP synthase. *Proc. Natl. Acad. Sci. USA* **98**, 898–902 (2001).
38. Ueno, H., Nishikawa, S., Iino, R., Tabata, K. V., Sakakihara, S., Yanagida, T. & Noji, H. Simple dark-field microscopy with nanometer spatial precision and microsecond temporal resolution. *Biophys. J.* **98**, 2014–2023 (2010).
39. Han, J. & Burgess, K. Fluorescent indicators for intracellular pH. *Chem. Rev.* **110**, 2709–2728 (2010).
40. Rosing, J., Kayalar, C. & Boyer, P. D. Evidence for energy-dependent change in phosphate binding for mitochondrial oxidative-phosphorylation based on measurements of medium and Intermediate phosphate-water exchanges. *J. Biol. Chem.* **252**, 2478–2485 (1977).